

Article

A Probabilistic Approach for the Optimal Sizing of Storage Devices to Increase the Penetration of Plug-in Electric Vehicles in Direct Current Networks

Elio Chiodo ¹ , Maurizio Fantauzzi ¹, Davide Lauria ¹ and Fabio Mottola ^{2,*} 

¹ Department of Industrial Engineering, University of Naples Federico II, Naples 80125, Italy; elio.chiodo@unina.it (E.C.); maurizio.fantauzzi@unina.it (M.F.); davide.lauria@unina.it (D.L.)

² Department of Engineering, University of Naples Parthenope, Naples 80143, Italy

* Correspondence: fmottola@unina.it

Received: 31 March 2018; Accepted: 11 May 2018; Published: 13 May 2018



Abstract: The growing diffusion of electric vehicles connected to distribution networks for charging purposes is an ongoing problem that utilities must deal with. Direct current networks and storage devices have emerged as a feasible means of satisfying the expected increases in the numbers of vehicles while preserving the effective operation of the network. In this paper, an innovative probabilistic methodology is proposed for the optimal sizing of electrical storage devices with the aim of maximizing the penetration of plug-in electric vehicles while preserving efficient and effective operation of the network. The proposed methodology is based on an analytical solution of the problem concerning the power losses minimization in distribution networks equipped with storage devices. The closed-form expression that was obtained is included in a Monte Carlo simulation procedure aimed at handling the uncertainties in loads and renewable generation units. The results of several numerical applications are reported and discussed to demonstrate the validity of the proposed solution. Also, different penetration levels of generation units were analyzed in order to focus on the importance of renewable generation.

Keywords: energy storage; design optimization; plug-in electric vehicles; energy efficiency

1. Introduction

In efforts to ensure sustainable societies, smart technologies have been identified as significant contributors to meet the expected increment of energy that will be required due to the human activities in urban areas [1,2]. Different aspects of human life related to the traditional consumption of electricity must be considered, including both the residential and commercial demands for heat, air conditioning, mobility (e.g., public and private transportation systems), and communication systems (e.g., smart phones, tablets, and servers). Users will have to be managed as integrated systems aimed at making the use of the energy more efficient [2–7]. Focusing on mobility, the owners of plug-in electric vehicles (PEVs) have to connect their vehicles to distribution networks to charge the on-board batteries. This implies significant increases in the electrical load demand [8,9]. As a result, network power losses, line currents, and bus voltages could exceed admissible values, so either the networks must be upgraded or the actual load supplied must be curtailed. Various solutions have been proposed in the literature to deal with the increased load that will result from the electricity demand [9–35].

The main approaches for dealing with this issue that has been discussed to date deal with the coordinated charging of multiple PEVs in (1) a fleet of vehicles plugged into the grid through charging stations and (2) vehicles plugged into chargers connected at different locations in the distribution grids [9–14].

Another approach considered in the literature to deal with the increased use of PEVs is to focus on the use of electrical energy storage systems (EESSs). Such systems have proven useful in mitigating the impact of fast chargers on distribution networks and in reducing the operational costs [15–35]. An economic analysis of the use of a battery energy storage system in a charging station and its related advantages are discussed in [15]. As discussed in [16], EESSs can be useful in both standalone and grid-connected applications; in the first case, PEVs can be recharged by the power stored in the EESS, and, in the second case, the charging power can be delivered by either the EESS or the grid, based on the available stored energy and the optimal power flow requirements. In [17] and [18], EESSs were used for grid-connected, fast-charging stations equipped by renewable sources with a control system that acts on both the state of charge of the EESS and the value of the voltage at the connection-bus. In [19], an energy management system was proposed for the optimal operation of the electrical system of a building equipped by a storage system in order to meet the power requirements of a fleet of electric vehicles, renewable generation systems, and loads. The use of storage devices to reduce the peak power demand was proposed in [20,21]. The storage devices in charging stations are also used with the aim of reducing the total costs [22–26] and to optimize the management of energy consumption [27]. The coordination of chargers with EESSs has been used for voltage support in distribution feeders [28]. In [29], the storage device was used to deal with the impact of charging electric vehicles on the voltages and currents of a distribution feeder. In [30], the storage device was used in a charging system with the aim of exploiting the use of power generated by renewable energy sources. The utilization of distributed energy storage systems was proposed in [31,32] to alleviate the impacts of PEVs and generation units on distribution systems. The design and control of power converter systems for the charging infrastructures with integrated energy storage devices were discussed in [33–35].

Focusing on the solution discussed in [15–35], in this paper, the use of EESSs is proposed for the optimal integration of charging PEVs connected at the different buses of a distribution network. The use of storage devices is aimed at increasing the potential of the distribution network for supporting the increased penetration of PEVs. In more detail, an analytical-probabilistic procedure is presented for the optimal sizing of the EESS aimed at balancing load demand and renewable-based generation while (i) satisfying the network constraints and (ii) increasing the efficiency by minimizing power losses. The uncertainties in load demand, charging requests for PEVs, and renewable power production are included in the proposed analysis. Considering the applications in modern distribution grids, the use of DC networks to connect distributed resources is considered. In fact, DC systems are expected to have an important role in modern distribution networks because they allow integrating loads and renewable energies in a better and more efficient way. This is justified by considering several aspects related to both the intrinsic advantages of DC and the nature of loads and generation sources of modern electrical systems [36,37]. Typically, the following advantages generally are associated with DC systems:

- due to the absence of reactive power, DC systems provide more efficient service than alternating current (AC) systems in terms of reduction of power losses and voltage drops;
- the power produced by renewable energy sources is DC or requires the connection of power converters to the network (e.g., photovoltaic (PV) systems, wind turbines (WTs), and fuel cells);
- most loads operate with DC (e.g., lighting, PEVs, and computers).

With specific reference to PEVs, it must be considered that DC networks are the most favorable infrastructures to integrate fast PEV chargers [38,39]. In fact, fast chargers allow charging the on-board batteries in a short time (typically 15–30 min) by supplying DC power directly (typically 50–100 kW). Thus, the use of DC networks instead that AC networks avoids the use of AC/DC power conversion systems at each charger unit.

The problem of the optimal sizing of energy storage devices to be used to improve the integration of fast chargers for PEVs has been addressed in the recent literature [23–31]. In [23], the size of the storage device that is supporting a fast-charging station is determined by using mixed-integer,

nonlinear programming aimed at reducing the total costs. In [24], a stochastic optimization is proposed for a grid-connected charging station to determine the sizes of both the battery and the renewable generation system that allow the chargers to minimize the total cost. Based on the expected charging demand, in [25], a mixed-integer, linear-optimization problem was proposed to determine the optimal storage size in order to minimize the investment and operating costs in the planning horizon. In [26], a linear programming method was proposed to identify the optimal size of energy storage with the aim of reducing the daily operational costs of a fast charging station. In [27], a design methodology was proposed that can determine the optimal size of the storage device by maximizing the net present value of the profit derived from a charging station. In [28], a sizing method was proposed based on mixed integer linear programming for EESSs used to provide voltage support in feeders with PV systems. In [29], an augmented time-series energy balance was used to determine the size of the battery in a charging station that would reduce the impact of the chargers on the electrical network; the author used a chance constraint-based method to deal with the uncertainties in the network's load, generation, and the number of PEVs. In [30], a search-based algorithm was used to solve the problem of determining the optimal storage sizing, and it was formulated in terms of the mixed integer optimization problem aimed at satisfying the load demand entirely by renewable energy sources. A Markov chain model was used to account for the intermittency in renewable generation. In [31], two interdependent sub-problems were formulated and solved by using both metaheuristic and deterministic optimization techniques with a general objective function that deals with the total annual cost of energy. The uncertainties associated with the demand for the charging of PEVs and with the generation of renewable units were considered through a Markov chain Monte Carlo simulation model.

The probabilistic procedure proposed in this paper uses a Monte Carlo-based method that applies an analytical optimization of different EESSs iteratively in DC networks in the presence of renewable-based, distributed generation (DG) units and PEVs. The analytical formulation was based on the general methodology presented in [40], which allows determining the sizes of the EESSs that would be required to minimize the grid power losses. Among different scenarios characterized by different penetrations of PEVs and DG units, the sizes of EESSs have been derived from the results of the Monte Carlo simulation procedure which is widely adopted for statistical studies [41]. Then, the choice of the optimal size of EESSs is derived on the basis of the satisfaction of the network's constraints (e.g., bus voltages and line currents).

Compared to the current literature on this topic, the main contributions of the proposed method are:

- the optimal sizing of EESSs in DC networks with the aim of increasing the number of PEVs that can be charged while satisfying constraints related to the network operation;
- the proposed sizing method is specifically tailored for the case of DC networks and the infrastructures for the fast charging of PEVs that have been identified as the key infrastructures of future distribution grids;
- the ability of the proposed method to manage the complexities related to the multiple uncertainties in the demands for renewable energy and PEVs in a feasible and accurate manner by including the analytical, optimal sizing of EESSs within a procedure based on the Monte Carlo method.

Note that the method presented here for the general case of distribution networks easily can be applied to charging stations. Thus, the method can be used for the cases of both distributed and centralized EESSs.

The rest of the paper is organized as follows: the optimal sizing procedure is proposed in Section 2. Section 3 reports the results of numerical applications referred to different scenarios; in particular, different penetration levels of renewable generation are analyzed. For each scenario, we analyzed the indices that typically are used to measure the impact of PEVs on the network. Our conclusions are presented in Section 4.

2. The Probabilistic Sizing Method

In this section, we provide details concerning the proposed probabilistic method aimed at maximizing the penetration of PEVs in DC distribution networks through the use of distributed EESSs. Our definition of the penetration of PEVs is the total number of PEVs that can be connected to the DC network for charging purposes.

The inputs required for the procedure are the network topology, the buses at which the PEV chargers and EESSs can be connected, the profiles of the power requested from the loads and the power produced by the DG units with reference to the planning time horizon. The inputs include the statistical characterization of the uncertainties of load demand, the production of the DG units, and charging requests for PEVs over the specified time horizon. In the case of PEVs, statistical characterization refers to the time of arrival and the corresponding energy request. More specifically, with reference to a specified time interval, all of the uncertain quantities are handled as random variables, each characterized by a specific probability density function (pdf).

The outputs of the proposed method are the maximum penetration of PEVs and the corresponding optimal sizes of the EESSs that allow balancing load and generation efficiently and satisfying the constraints of the network. These outputs are derived based on the pdfs of the line currents, bus voltages, imported power and EESSs sizes resulting from the application of the Monte Carlo procedure. The constraints considered were: (i) the power imported by the grid, (ii) the line currents, and (iii) the bus voltages.

The proposed method can be described in the following three steps (Figure 1):

- 1) The Monte Carlo simulation procedure is applied to the initial penetration of PEVs, specifically:
 - 1.1. Starting from the known pdfs, N_s samples of the power profiles of loads, PEV chargers, and DG units are identified over the specified planning time;
 - 1.2. A deterministic optimization procedure is applied at each sample, and the results are used to determine the optimal energy capacity of the EESSs required to balance load demand and power production while minimizing network power losses;
 - 1.3. Collect the N_s samples of the energy capacity of the EESSs and the corresponding profiles of line currents, bus voltages, and power imported by the DC network.
- 2) Increase the penetration of PEVs and repeat the Monte Carlo simulation (point 1).
- 3) After points 1 and 2 are performed for all of the PEV penetration levels, the statistical characterizations of currents, voltages, and power imported are analyzed, and, finally, the sizes of the EESSs are chosen as those that can satisfy the constraints imposed by the considered DC network.

The computational burden of the proposed probabilistic framework should not be discouraging. Indeed, the main complex computational task is the solution of the sizing of the EESSs, which is derived in analytical terms. Hence, a closed form solution is used (as discussed in Section 2.2) that makes it possible to manage the vast amount of uncertainties, and it easily can be extended to provide further optimization variables (e.g., the penetration of the renewable generation or the location of both EESSs and PEVs chargers).

The proposed method is detailed below. The statistical characterizations of the uncertain quantities (power profiles of loads, PEVs, and DG units) are discussed first. Then, the deterministic optimal procedure used to evaluate the EESSs capacity at each iteration of the Monte Carlo procedure is presented briefly. Finally, we discuss the analysis of the statistical characterization of the outputs and the procedure to evaluate the maximum penetration of PEVs and the corresponding optimal sizes of the EESSs.

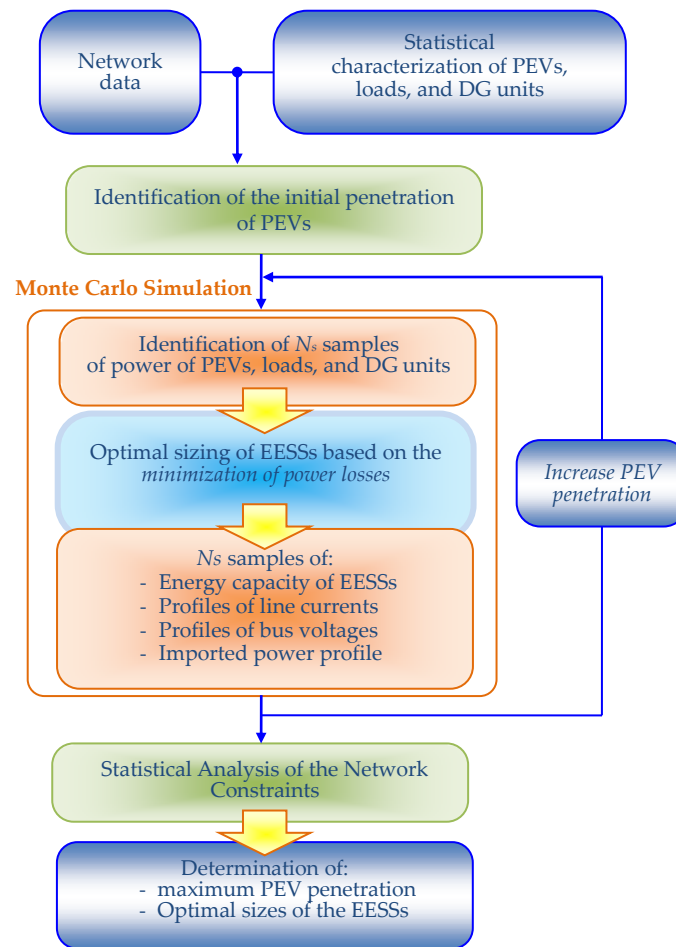


Figure 1. Flow chart of the proposed probabilistic method.

2.1. Assumptions Concerning the Statistical Characterization of Uncertainties

In order to apply the proposed method, a reference work cycle for the EESSs must be defined. The reference work cycle was considered to be one day, and it was divided into time steps of duration, Δt . In order to consider the uncertainties at each time step, the values of power injected by the DG units and the power required by the loads and PEVs are managed as random variables, each of which was characterized by the proper pdfs (Figure 2).

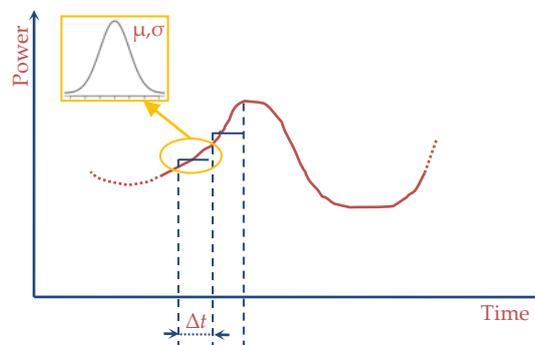


Figure 2. Qualitative representation of the statistical characterization of the electrical power of loads, PEVs, and the DG unit.

Based on different probabilistic models, different types of pdf can be used, such as Normal or the Lognormal pdf [42–44]. Discussion of the most accurate pdf is out of the scope of this paper. In the numerical application, the case of Normal pdf was assumed for the power for both the DG units and the loads. Obviously, different distributions easily can be used in the proposed approach.

Regarding the statistical characterization of PEVs, there are difficulties associated with the randomness of both the arrival time and the energy required for charging the on-board batteries. Different models can be used to manage these random values [45,46]. The arrival time and the desired charge level can be assumed to have proper pdf. However, to provide a statistical characterization of the power request of the PEVs connected to the grid, details concerning the chargers used for the PEVs also are needed, and the strategy that will be used for the charging must be specified. In this paper, the following process, $W(t)$, is used to define the power requested by the chargers:

$$W(t) = \sum_{k=1}^{N_{pev,p}} W_k(t, \vartheta_k, T_k), \quad (1)$$

where, with reference to the k^{th} PEV to be connected at bus p , $W_k(t, \vartheta_k, T_k)$ is a “Window” function of time of a given amplitude, $A(t)$, which represents the power requested by the vehicle’s charger, and duration, ϑ_k , starting at a random arrival time, T_k , i.e.:

$$W_k(t, \vartheta_k, T_k) = \begin{cases} A(t) & T_k \leq t \leq \vartheta_k \\ 0 & otherwise \end{cases}, \quad (2)$$

In order to manage the power requested by the PEV chargers, different pdfs of $A(t)$, ϑ_k , and T_k can be used. In the numerical applications of this paper, it was assumed that, when the vehicle is plugged in, the PEV charger absorbs its rated power starting from when the PEV is plugged in and ending when the on-board battery is fully charged; a uniform distribution is assumed for the arrival time. Obviously, this is just an assumption, and different and more accurate distributions for the arrival time and energy requests easily can be implemented.

2.2. Analytical Evaluation of the Optimal Sizing of the EESSs

In this sub-section, the formulation of the problem concerning the minimization of power losses in DC networks and its analytical solution in presence of EESSs are repeated briefly based on reference [40]. The solution of this minimization problem provides the optimal energy capacity to be requested of the EESSs connected to the grid. This solution is provided in terms of a closed form expression. The DC network is assumed to be connected to the main distribution grid at a point of common coupling. At this stage, PEVs can be regarded as loads, and the presence of other loads, DG units, and EESSs is considered. Thus, the problem refers to a multi-period minimization problem over a time horizon T , which is formulated as:

$$\min P_{loss}(t) \quad (3)$$

subject to:

$$\mathbf{J}(t) = \mathbf{G} \mathbf{V}(t) \quad \forall t \in [0, T] \quad (4)$$

$$\int_0^T \text{diag}(\mathbf{V}_{ES}(t)) \mathbf{J}_{ES}(t) dt = \mathbf{0} \quad (5)$$

where $P_{loss}(t)$ is the power losses at time t ; $\mathbf{J}(t)$ is the vector of current injected at all of the network buses at time t ; $\mathbf{V}(t)$ is the vector of bus voltages at time t ; \mathbf{G} is the conductance matrix of the DC network; diag indicates the diagonal matrix; and $\mathbf{V}_{ES}(t)$ and $\mathbf{J}_{ES}(t)$ are, with reference to time t , the voltage and the injected currents, respectively, at the buses where the EESSs are connected. In this paper, the values assumed by the quantities refer to the standard international units except for the energy for which

Wh (or kWh) is used. Equation (4) refers to the power balance in the DC network, and Equation (5) refers to the balance of the energy stored in each of the EESSs, and both of the equations refer to the one-day work cycle of the EESSs, T . Based on the values of power requested, the currents injected in buses where DG and loads are connected easily can be derived as functions of the bus voltage. The balance Equation (5), allows the inclusion of an isoperimetric constraint that can be managed analytically in the proposed minimization problem. In particular, based on a generalized matrix model of the DC network and on a linear approximation of the load flow Equation (4), a generalized methodology for the analytical solution of the minimization problem, Equations (3)–(5) was proposed in [40]. Thus, a suitable network's resistance matrix can be built with the aim of providing the calculus of the network's power losses as a function of the nodal injected currents. To do that, let the point of common coupling be the slack bus (bus #0) and the remaining busses classified as load busses (including the PEV chargers) $(1, \dots, n_L)$, DG busses $(n_L + 1, \dots, n_L + n_G)$ and the EESS busses $(n_L + n_G + 1, \dots, n)$. The voltage of the slack bus is assumed to have a specified constant value, E . In this case, the DC network can be described through a matrix formulation as:

$$\begin{bmatrix} J_0(t) \\ \mathbf{J}^*(t) \end{bmatrix} = \mathbf{G} \begin{bmatrix} E \\ \mathbf{V}^*(t) \end{bmatrix} \quad (6)$$

where, with reference to the time t , $J_0(t)$ is the current injected at the slack bus (which is an unknown variable), $\mathbf{V}^*(t)$ and $\mathbf{J}^*(t)$ are the vectors of the voltages and currents injected at the remaining buses of the network. By partitioning matrix \mathbf{G} , the following equation can be derived:

$$\begin{bmatrix} J_0(t) \\ \mathbf{J}^*(t) \end{bmatrix} = \begin{bmatrix} \mathbf{G}_{00}(t) & \mathbf{G}_{0E}(t) \\ \mathbf{G}_{E0}(t) & \mathbf{G}_{EE}(t) \end{bmatrix} \begin{bmatrix} E \\ \mathbf{V}^*(t) \end{bmatrix} \quad (7)$$

The sub-matrix, \mathbf{G}_{EE} , is not singular, so we can evaluate the bus voltages as:

$$\mathbf{V}^*(t) = E\mathbf{1} + \mathbf{R}\mathbf{J}^*(t) \quad (8)$$

where $\mathbf{1}$ is the vector of all ones, and $\mathbf{R} = \mathbf{G}_{EE}^{-1}$. Thus, a closed form expression for the network power losses can be derived as [40]:

$$P_{loss}(t) = \mathbf{J}^*(t)^T \mathbf{R} \mathbf{J}^*(t) \quad (9)$$

Based on the linear approximation of the power flow solution proposed in [47], the corresponding bus voltages can be obtained from the following linear approximation:

$$\mathbf{V}^*(t) = E\mathbf{1} + \frac{\mathbf{R}\mathbf{P}^*(t)}{E} \quad (10)$$

where:

$$\mathbf{P}^*(t) = \text{diag}(\mathbf{J}^*(t)) \mathbf{V}^*(t) \quad (11)$$

By representing matrix \mathbf{R} as:

$$\mathbf{R} = \begin{bmatrix} \mathbf{R}_{11} & \mathbf{R}_{12} \\ \mathbf{R}_{21} & \mathbf{R}_{22} \end{bmatrix} \quad (12)$$

the following linear expression can be derived from Equation (10):

$$\mathbf{V}^*(t) = E\mathbf{1} + \mathbf{R}_{11} \frac{\mathbf{P}^*(t)}{E} + \mathbf{R}_{12} \mathbf{J}_{sto}(t) \quad (13)$$

In the case of the approximated expression in Equation (13), in [40], an analytical solution of the minimization problem (3)–(5) was derived as:

$$\mathbf{J}_{sto}(t) = -\mathbf{B}_1(t) \cdot \mathbf{K}_1(t) + \mathbf{B}_2(t) \left[\int_0^T \mathbf{B}_2(t) dt \right]^{-1} \int_0^T \mathbf{B}_1(t) \cdot \mathbf{K}_1(t) dt \quad (14)$$

where:

$$\mathbf{B}_1(t) = [\mathbf{A}_1(t)\mathbf{K}_2(t) + \mathbf{A}_2(t)]^{-1}\mathbf{A}_1(t) \quad (15)$$

$$\mathbf{B}_2(t) = \frac{1}{2}[\mathbf{A}_1(t)\mathbf{K}_2(t) + \mathbf{A}_2(t)]^{-1} \quad (16)$$

$$\mathbf{A}_1(t) = \mathbf{K}_2^T(t)\mathbf{R}_{11} + \mathbf{R}_{21} \quad (17)$$

$$\mathbf{A}_2(t) = \mathbf{K}_2^T(t)\mathbf{R}_{12} + \mathbf{R}_{22} \quad (18)$$

with:

$$\mathbf{K}_1(t) = \frac{1}{E} \text{diag}(\mathbf{P}^*(t)) \left(\mathbf{I} - \frac{\mathbf{R}_{11}\mathbf{P}^*(t)}{E^2} \right) \quad (19)$$

$$\mathbf{K}_2(t) = -\frac{1}{E^2} \text{diag}(\mathbf{P}^*(t)) \mathbf{R}_{12} \quad (20)$$

Once the vectors of the current and voltage profiles at the busses of the EESSs have been derived, the energy capacity requested for the EESSs easily can be derived as:

$$E_{ES,q} = \max_{t \in [0,T]} \left(\int_0^t V_{sto,q}(\tau) J_{sto,q}(\tau) d\tau \right) - \min_{t \in [0,T]} \left(\int_0^t V_{sto,q}(\tau) J_{sto,q}(\tau) d\tau \right) \quad \forall q \in \Omega_{ES} \quad (21)$$

where $E_{ES,q}$ is the requested energy capacity of the EESSs connected at the bus q , and Ω_{ES} is the set of buses where the EESSs are connected. Based on the storage technology and desired lifetime, the sizes of the EESSs can be derived from Equation (21). Through the voltage profiles at all of the buses, which are given by Equation (13), the line currents at all of the time intervals can be derived.

It is worth to remark that, in this paper, the solution provided by Equation (21) is used to derive the energy capacity for all of the EESSs and for each of the iteration of the Monte Carlo simulation procedure. At each iteration, the uncertainties affecting the solution Equation (21) are the power profiles of loads, PEVs' chargers and DG units which can be treated as random variables, as discussed in Section 2.1. The application of this approach, allows deriving the pdfs of the energy capacities and other electrical quantities related to the network operation (e.g., line currents and bus voltages). These pdfs can be managed to derive the correct sizes of the EESSs that allows maximizing network efficiency (since Equation (21) is the solution of a network's losses minimization problem) while satisfying network constraints. This last aspect is detailed in the Section 2.3.

2.3. Derivation of the Maximum Penetration of PEVs and Related Sizes of the EESSs

With reference to a specified penetration level of PEVs, by applying the sizing procedure of Section 2.2 within the Monte Carlo simulation procedure, N_s samples of the outputs (i.e., profiles of line currents, bus voltages, imported power, and the capacities of the EESSs) were derived. This allowed us to obtain the statistical characterization of these quantities that can be managed through their sample pdf and related parameters, such as their means, medians, or percentiles. These data can be collected for each specified penetration of PEVs. Among these collected data, the maximum value of the penetration of the PEVs and the corresponding optimal capacity of the EESSs were derived as those that, in statistical terms, allow satisfying the network constraints on voltages, currents, and

imported power. Then, the maximum allowable penetration of PEVs (PEV^{\max}) can be expressed in mathematical terms as:

$$PEV^{\max} = \sum_{p \in \Omega_{pev}} N_{PEV,p} \quad (22)$$

such that:

$$\hat{v}_i(t) \leq V_{\max} \quad i = 1, \dots, n \quad \forall t \in [0, T] \quad (23)$$

$$\hat{v}_i(t) \geq V_{\min} \quad i = 1, \dots, n \quad \forall t \in [0, T] \quad (24)$$

$$\hat{j}_j(t) \leq J_{j,\max} \quad j = 1, \dots, l \quad \forall t \in [0, T] \quad (25)$$

$$\hat{p}_1(t) \leq P_{1,\max} \quad \forall t \in [0, T] \quad (26)$$

where $N_{PEV,p}$ is the number of PEVs connected at the p^{th} bus; Ω_{pev} is the set of buses where chargers for PEVs are connected; n is the total number of busses in the network; l is the total number of lines in the network; $\hat{v}_i(t)$ is the value of a specified parameter (e.g., mean, median, or percentile) of the pdf of the voltage related to the i^{th} bus and time t ; V_{\min} and V_{\max} are the minimum and maximum values, respectively, allowed to the bus voltages; $\hat{j}_j(t)$ is the value of a specified parameter (e.g., mean, median, or percentile) of the current pdf related to the j^{th} line and time t ; $J_{j,\max}$ is the ampacity of the j^{th} line of the network; $\hat{p}_1(t)$ is the value of a specified parameter (e.g., mean, median, or percentile) of the pdf of the power imported by the network at time t ; $P_{1,\max}$ is the maximum power that can be imported from the main distribution grid.

To choose the correct value of the energy capacity, different approaches can be used to manage the pdf of the random variables statistically characterized through the proposed Monte Carlo-based method. As an example, if the percentiles of the outputs are considered, errors in the forecasting could be considered within the sizing procedure. In the numerical application of this paper, the outputs of the proposed procedure (i.e., maximum number of PEVs and corresponding capacity of EESSs) were chosen on the basis of the mean values of the pdf used in the (22)–(26).

3. Numerical Applications

The proposed approach was tested on the LV DC test network shown in Figure 3. This network was adapted from the AC LV CIGRE distribution network [48] and used to be operated in DC 400 V, as discussed in [40].

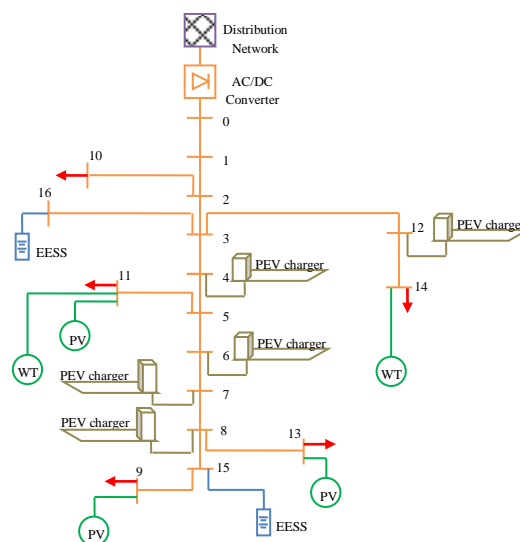


Figure 3. Test DC network in this study.

The locations and rated powers of the loads and DG units considered in this application are reported in Table 1. Regarding the PEVs, five vehicle chargers were connected at buses #4, #6, #7, #8, and #12, all of which were fast chargers with 50 kW of rated power [38]. It was assumed that the chargers could fully charge one PEV in one hour.

Table 1. Location and rated powers of loads and DG.

Load		DG		
Bus #	Rated Power [kW]	Bus #	Typology	Rated Power [kW]
9	20	9	PV	5
10	5	11	PV	5
11	20	13	PV	5
13	5	11	WT	10
14	25	14	WT	5

The day was divided in 24 intervals for which normal pdfs were assumed for the power of the loads and the DG units. An example of a load is shown in Figure 4, where the mean values at each hour are reported with reference to bus #10. An example of the hourly mean values of DG power production is shown in Figure 5 with reference to the PV system located at bus #14. The standard deviation of both the loads and DG unit were derived using a constant coefficient of variation of 10%.

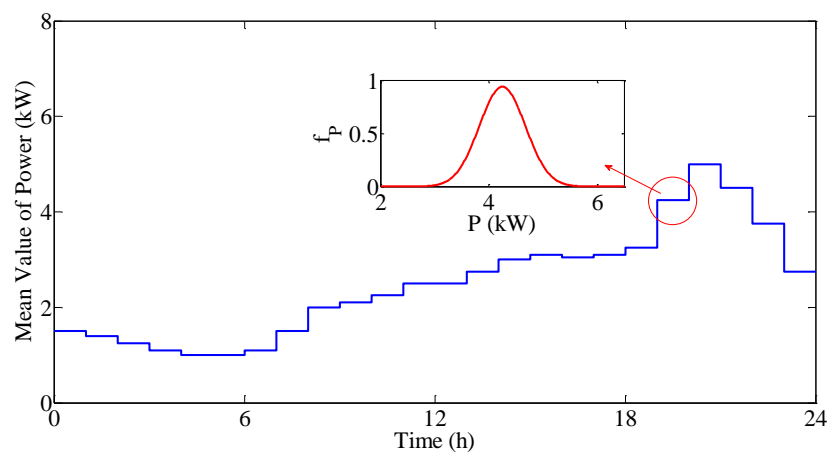


Figure 4. Hourly mean values of the power absorbed at bus #10.

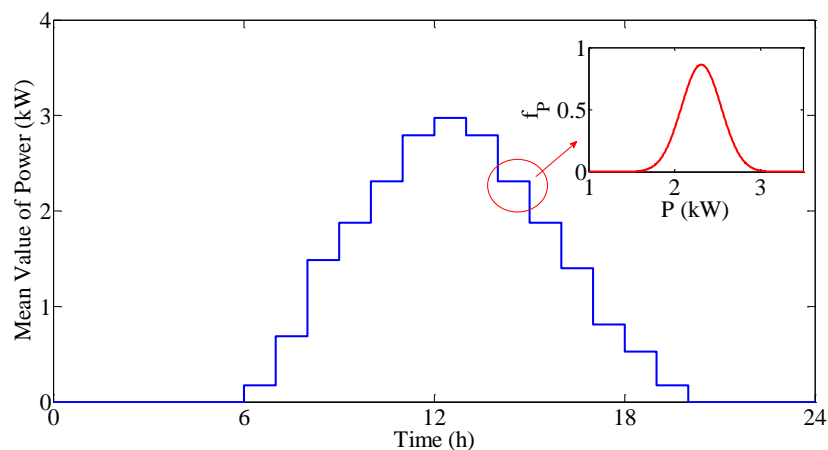


Figure 5. Hourly mean values of the power produced by the PV unit at bus #14.

Regarding the charger for the PEVs, two types of customers were assumed:

- *residential customers*: PEVs are connected to the chargers mainly during the evening and night hours (buses #4, #7, and #8);
- *commercial customers*: PEVs are connected to the chargers mainly during the hours in the morning and in the middle of the day (buses #6 and #12).

For both types of customers, we assumed uniform pdf to determine the specific arrival times.

Two EESSs can be connected at buses #15 and #16, and their energy capacities would be optimized through the proposed procedure. The procedure was used for increasing numbers of PEVs connected at buses equipped with chargers. The results of the simulation are reported in Figures 6 and 7. With reference to the expected number of PEVs, the average values of the lowest and highest bus voltages (per unit value of the nominal voltage) are shown in Figure 6. The average value of the highest value of the line currents (per unit value of the line ampacities) are shown in Figure 7. Cases with and without EESSs are reported in both figures. Figure 6 shows that the use of EESSs allowed increases in the number of PEVs to be charged without affecting the voltage values, which remained within the acceptable range (0.9–1.1 p.u.). The absence of the EESSs, instead, implies a negative impact on the bus voltage when the number of PEVs was larger than 40. Figure 7 shows that the maximum admissible line currents were attained in both cases, i.e., with and without EESSs. Thus, the maximum number of PEVs that can be charged must be lower than 25 vehicles when EESSs are used, while only few vehicles could be charged when no EESSs were connected.

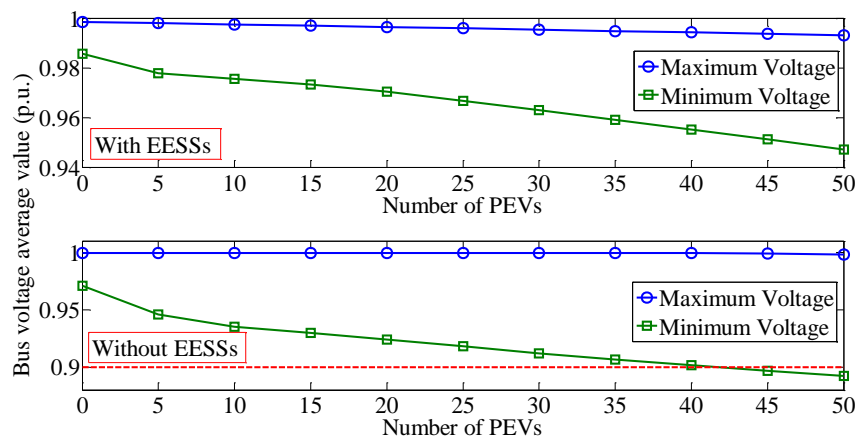


Figure 6. Minimum and maximum bus voltage average value for different number of PEVs with and without EESSs.

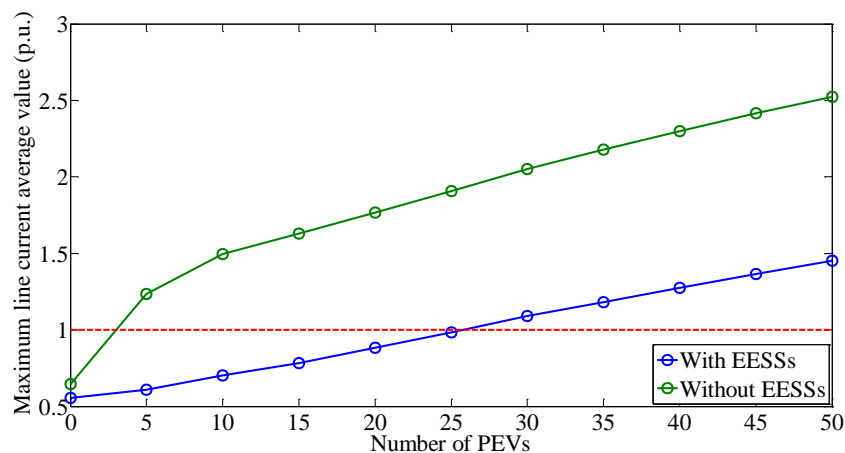


Figure 7. Maximum line current average value for different number of PEVs with and without EESSs.

Figure 8 shows the average values of the energy capacity requested by the EESSs for different penetrations of PEVs (i.e., the number of PEVs). The figure shows that the EESS connected at bus #15 always required an energy capacity larger than the one connected at bus #16, and the disparity increased as the PEV penetration increased. In addition, the energy capacity relative to bus #16 was almost constant with variation of PEVs, meaning that the ability to satisfy a larger fleet of PEVs was due mainly to the increased capacity of the EESS located at bus #15. In Figure 8, the size has to be selected that corresponds to the maximum PEV penetration imposed by the constraint on line currents (Figure 7), which is slightly greater than 25. At this penetration level, the corresponding sample pdfs obtained for the capacity of both EESSs are reported in Figure 9, together with their average values (μ) and standard deviations (σ). Figure 9 clearly shows that the pdf of the EESS located at bus #15 was affected by the large demand of power requested for charging the batteries for the PEVs. However, the EESS at bus #16 mainly was needed to satisfy the service related to the other loads that were always present. In order to show the advantages obtained by the use of the EESSs in terms of energy efficiency, the power losses were compared for the cases with and without EESSs, and the results are reported in Figure 10.

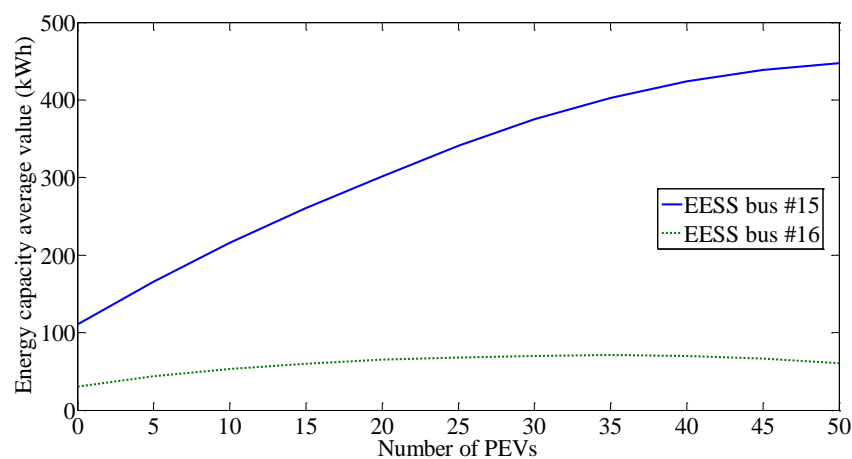


Figure 8. Energy capacity average value of the EESSs resulting from the sizing procedure for different number of PEVs.

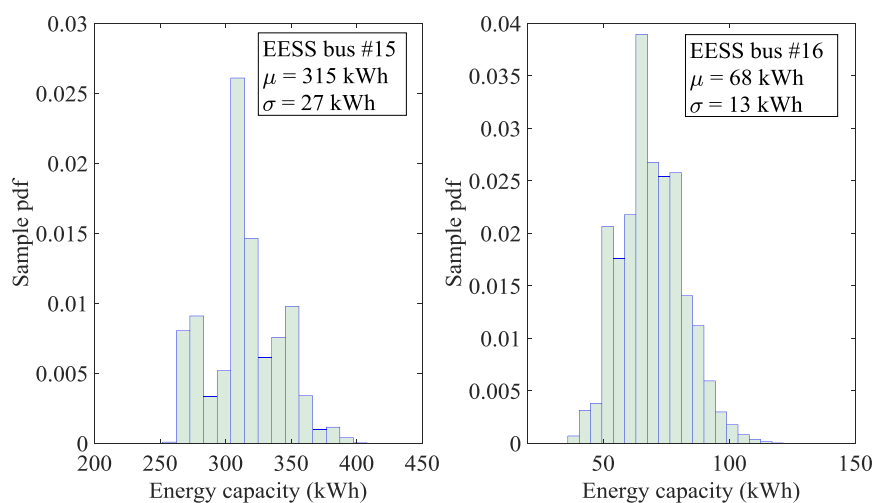


Figure 9. Sample pdf of the energy capacity requested to the EESSs corresponding to the case of maximum allowed number of PEVs.

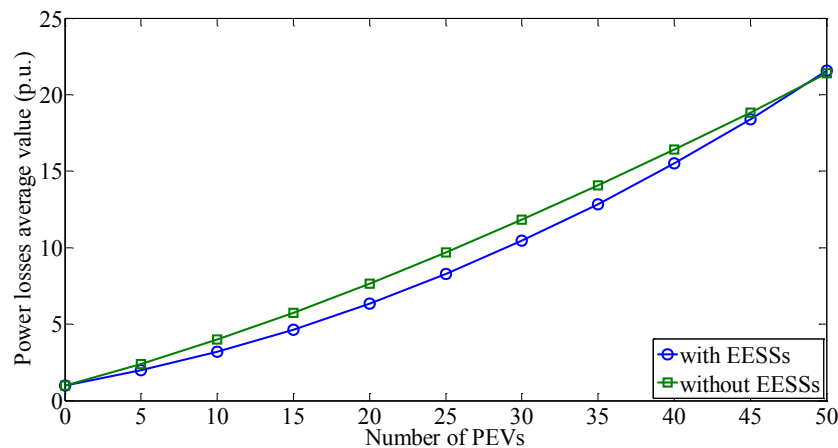


Figure 10. Average value of the power losses for different number of PEVs.

Figure 11 shows the average values of the peak demand of the power imported from the upstream grid. In Figures 10 and 11, the curves refer to different PEV penetrations and are reported in per unit of the corresponding values in the case of no PEVs being plugged in.

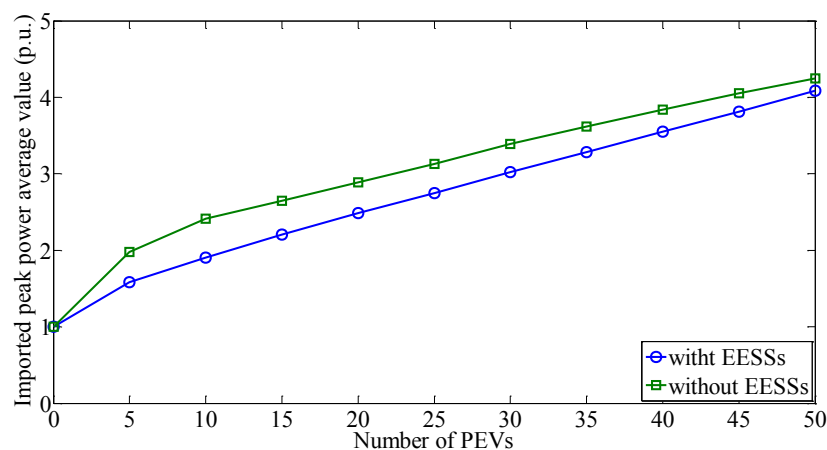


Figure 11. Average value of the imported peak power for different number of PEVs.

Figure 10 shows that the increased power losses that correspond to the increased penetration of PEVs can be mitigated by the use of EESSs. This effect clearly appears in correspondence of the maximum PEV penetration derived in Figure 7 (25 PEVs), while it is reduced when the number of PEVs increase. This effect was negligible for even higher values of PEV penetration. This confirms that grid efficiency can be increased if EESSs correctly sized are connected with the aim of improving the power balance of generation and loads while accounting for the satisfaction of the technical constraints of the grid (e.g., lines' ampacities). Figure 11 clearly shows how the presence of EESSs allows the peak power imported from the upstream grid to be reduced, even in presence of higher penetrations of PEVs.

By focusing on the solution of Figure 9 (size of the EESS located bus #15 is 315 kWh and the size of the EESS located at bus#16 is 68 kWh), the variation of the inputs has been verified by iteratively applying the analytical approach of Section 2.2. At this aim, 10,000 samples extracted from the pdfs of the inputs (powers of loads, PEVs and DG) have been used to evaluate the line currents and the bus voltages. The results of these simulations in terms of relative frequency of occurrences of the maximum line currents, minimum and maximum bus voltage values are summarized in Figures 12–14. In particular, Figure 12 reports the relative frequency of the maximum line currents, Figure 13 reports

the relative frequency of the minimum values of the bus voltages and Figure 14 refers to the bus voltage maximum values. In these figures, for comparative purposes, with reference to the same inputs, the results in absence of the EESSs are also reported.

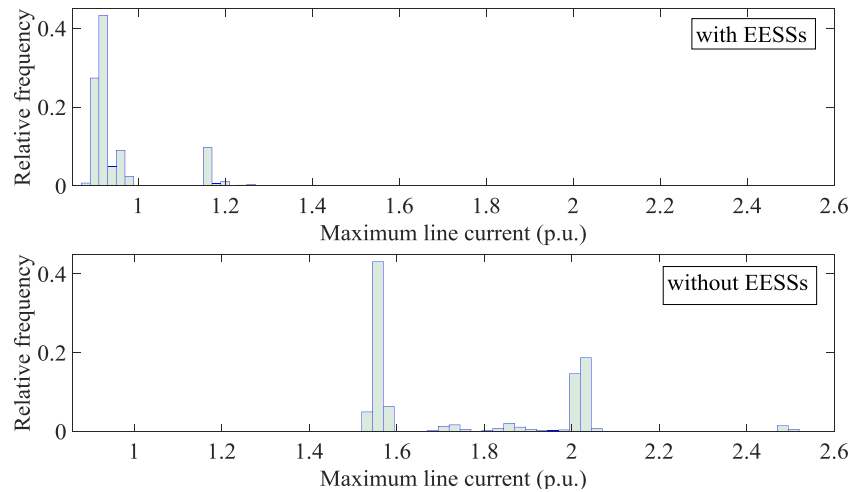


Figure 12. Relative frequency of occurrences of the maximum line current obtained with and without two EESSs (315 kWh @bus #15 and 68 kWh @bus #16).

Figure 12 shows that the use of properly sized EESSs allows satisfying the requested penetration level of PEVs by maintaining the line current within acceptable values. Only in few occurrences the current slightly exceeds the line ampacity (i.e., the current is greater than 1 p.u.), so requiring precautions in real time operation. At the designing stage, greater sizes of EESSs could be considered to reduce the number of these occurrences. As discussed in the Section 2.3, this could be done by sizing the EESSs through the use of specified values of the percentiles instead that the mean value.

By comparing the upper and lower histograms of Figure 12 (in both figures the same scale for the abscissa has been used), it is evident that, in absence of storage devices, the requested penetration level of PEVs cannot be satisfied, since their power demands always imply line maximum currents that exceed the lines' ampacities.

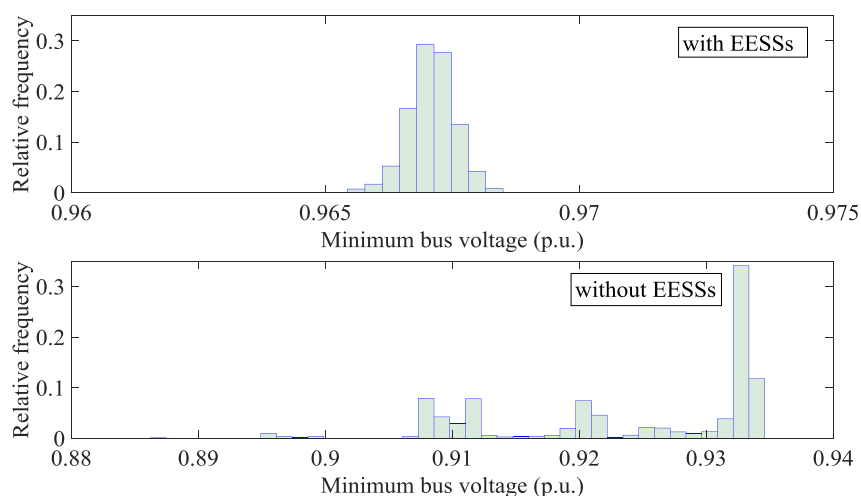


Figure 13. Relative frequency of occurrences of the minimum bus voltages obtained with and without two EESSs (315 kWh @bus #15 and 68 kWh @bus #16).

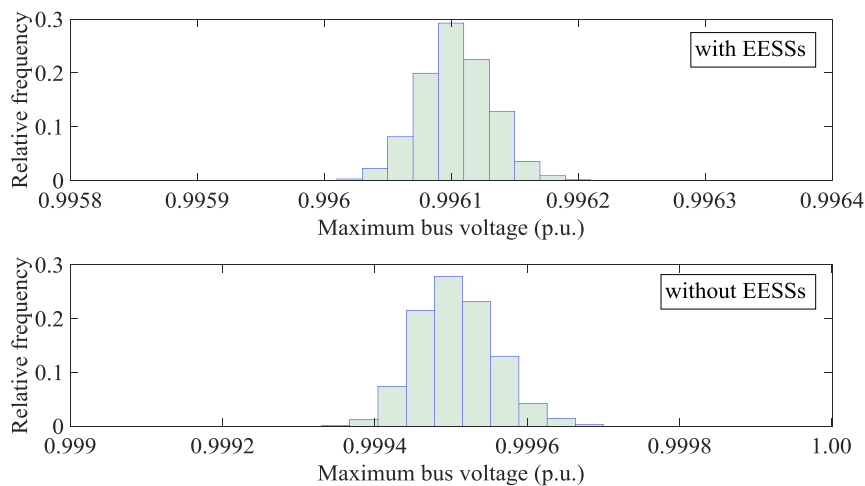


Figure 14. Relative frequency of occurrences of the maximum bus voltages obtained with and without two EESSs (315 kWh @bus #15 and 68 kWh @bus #16).

Figures 13 and 14 show that minimum and maximum voltage value always fall within the admissible range (0.9–1.1 p.u.) if the EESSs are used. In case of absence of storage devices, instead, in some circumstances the bus voltage values are lower than the admissible minimum limit. It has to be noticed that the shape of some histograms in Figures 12 and 13 are not unimodal, due to the fact that, in these cases, the limits imposed on currents or voltages are exceeded.

In order to study the impact of the penetration of renewable-based DG, we also considered the analysis of the increased values of both DG and PEV penetrations. Starting from the case of no DG, we considered increased values of the rated powers. The increased values of DG were evaluated in as a percentage of the rated power of Table 1. The maximum increment considered in the analysis was 300%. Figures 15 and 16 show the average values of the maximum bus voltages and line currents, respectively. In both figures, we used the per-unit values with respect to the nominal voltage (400 V) and the line ampacities.

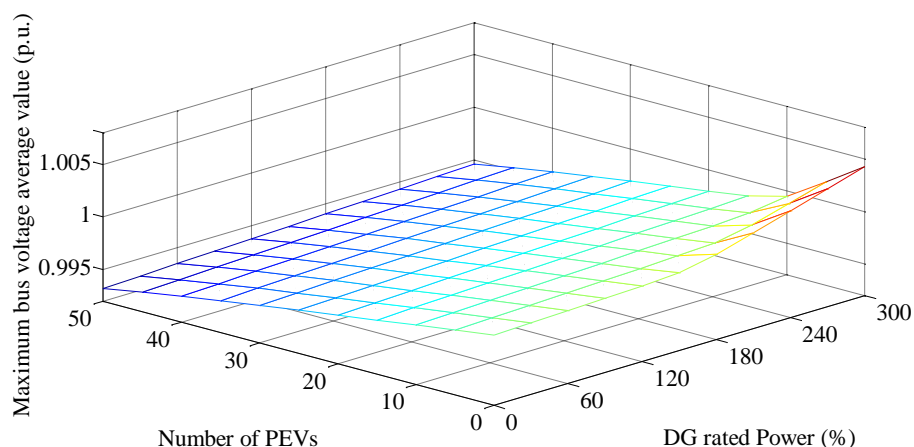


Figure 15. Maximum bus voltage average value for different number of PEVs and DG rated power.

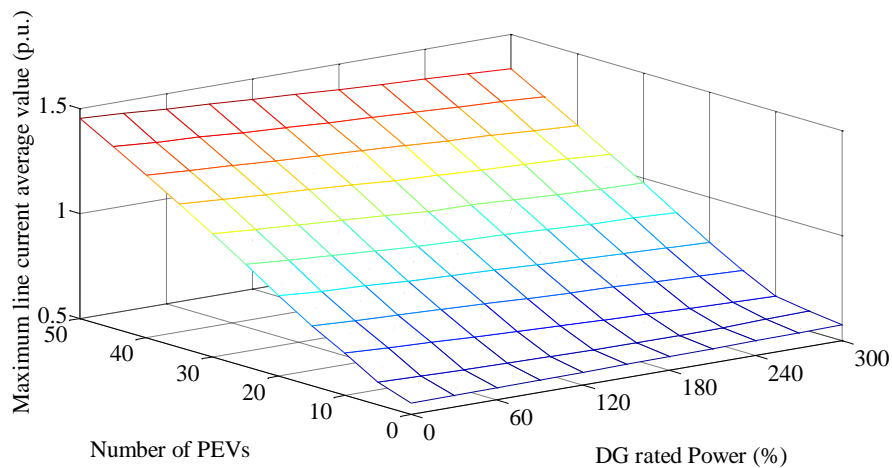


Figure 16. Maximum line current average value for different number of PEVs and DG rated power.

Figure 15 shows that the expected maximum voltage reached the highest values for the highest penetrations of DG units, while its lowest value was for the highest penetrations of PEVs. Figure 16 shows that the average maximum currents exceeded the line ampacities in the case of the highest penetrations of either DG or PEVs. To better highlight the limitations imposed by the constraint on the line currents, Figure 17 shows the average values of the maximum line currents versus DG rated powers and referred to different PEV penetrations. In Figure 17, note that a maximum penetration of 30 PEVs was allowed when the DG rated power was equal to or larger than 220%. In addition, increased levels of DG were unable to handle the increased demand of the PEVs because the constraint on the line current was never satisfied. This means that, to increase the penetration of PEVs, other structural modifications to the network must be made (e.g., by increasing the line ampacity). From Figure 17, it can be argued that by using storage devices with correct sizes, it is possible to improve the power balance between loads and generation in a more efficient way. Thus, increased penetration of PEVs can be satisfied by increased penetration of renewable-based DG units.

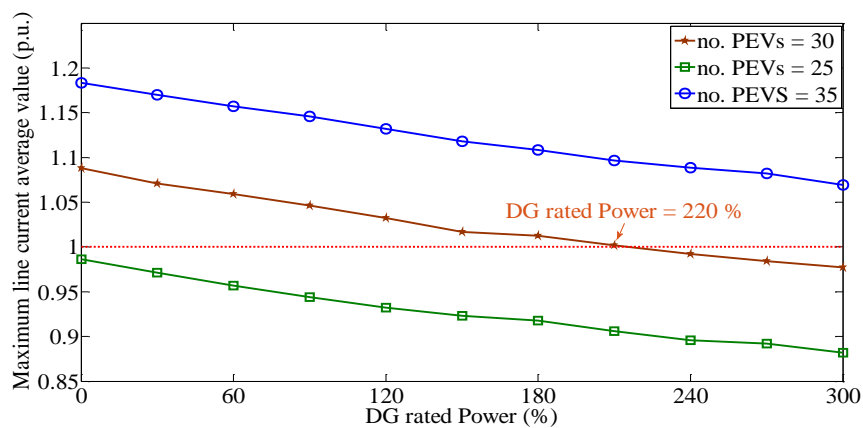


Figure 17. Maximum line current average value for different number of PEVs and DG rated power.

Figure 18 shows the sample pdf of the capacity requested to the EESSs in the case of the DG increment of 220% and 30 PEVs. The values of the EESSs also were able to reduce power losses and to decrease the peak power of the power imported from the upstream grid.

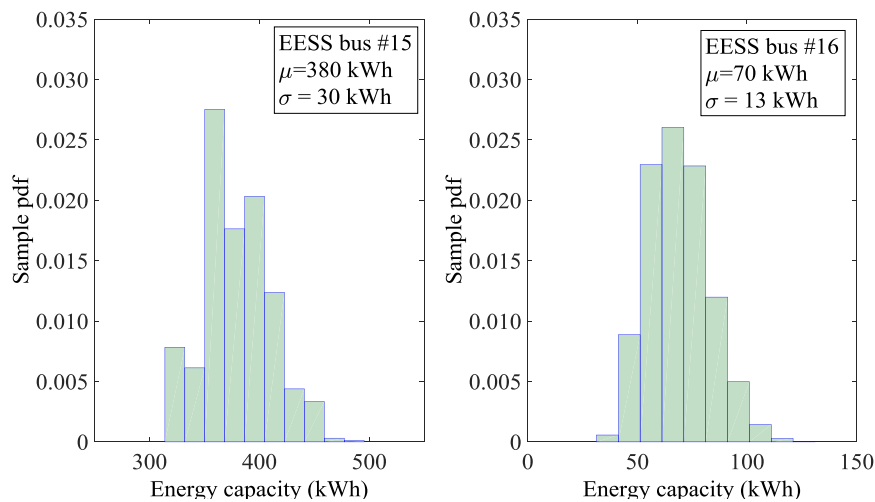


Figure 18. Sample pdf of the energy capacity requested to the EESSs corresponding to the case of maximum allowed number of PEVs.

4. Conclusions

A new probabilistic optimization methodology was proposed in this paper to manage unavoidable uncertainties in loads, PEVs and renewable production in DC distribution networks. The main goal of the proposed approach was the inclusion of an analytical tool within a Monte Carlo procedure. The stochastic approach takes into account all of the uncertainties of the problem, including the generation of renewable power, electric vehicles, and residential loads. Outputs of the procedure were the determination of the maximum penetration of PEVs and the corresponding optimal sizes of the EESSs that allow minimizing power losses while satisfying network constraints. The main advantage of the proposed method is that it contributes to the sustainable penetration of chargers for PEVs by encouraging the maximization of both the use of renewable energy resources and the efficiency of the operation of the grid. The proposed approach was tested on an LV DC test network to demonstrate the feasibility and key features of the method, i.e., how the increased power losses that correspond to increased penetration of PEVs can be mitigated by the use of EESSs. The results shown that increased PEVs' demand can be satisfied through the use of properly sized EESSs without including network modifications. Thus evidencing that the implementation of the proposed approach will allow designers to defer investments in grid reinforcement thereby reducing the negative impact of the rapid diffusion of PEVs, even in the presence of uncertainties. The proposed approach also was tested to verify the ability of DG to cope with the increased penetration of PEVs.

Author Contributions: All the Authors equally contributed to all the preparation activities of the work reported. E.C., M.F., D.L. and F.M. conceived and designed the solution methods and the case studies; E.C., M.F., D.L. and F.M. performed the numerical applications; E.C., M.F., D.L. and F.M. analyzed the data; E.C., M.F., D.L. and F.M. wrote the paper.

Funding: This research received no external funding.

Conflicts of Interest: The authors declare no conflict of interest.

References

1. Talari, S.; Shafie-khah, M.; Siano, P.; Loia, V.; Tommasetti, A.; Catalão, J.P.S. A Review of Smart Cities Based on the Internet of Things Concept. *Energies* **2017**, *10*, 421. [[CrossRef](#)]
2. Duarte, G.; Rolim, C.; Baptista, P. How battery electric vehicles can contribute to sustainable urban logistics: A real-world application in Lisbon, Portugal. *Sustain. Energy Technol. Assess.* **2016**, *15*, 71–78. [[CrossRef](#)]

3. Huang, S.; Infield, D. The impact of domestic Plug-in Hybrid Electric Vehicles on power distribution system loads. In Proceedings of the International Conference on Power System Technology, Hangzhou, China, 24–28 October 2010.
4. Akcin, M.; Kaygusuz, A.; Karabiber, A.; Alagoz, S.; Alagoz, B.B.; Keles, C. Opportunities for energy efficiency in smart cities. In Proceedings of the 4th International Istanbul Conference on Smart Grid Congress and Fair, Istanbul, Turkey, 20–21 April 2016.
5. Liu, N.; Chen, Q.; Liu, J.; Lu, X.; Li, P.; Lei, J.; Zhang, J. A Heuristic Operation Strategy for Commercial Building Microgrids Containing EVs and PV System. *IEEE Trans. Ind. Electron.* **2015**, *62*, 2560–2570. [[CrossRef](#)]
6. Acone, M.; Romano, R.; Piccolo, A.; Siano, P.; Loia, F.; Ippolito, M.G.; Zizzo, G. Designing an Energy Management System for smart houses. In Proceedings of the IEEE 15th International Conference on Environment and Electrical Engineering, Rome, Italy, 10–13 June 2015.
7. Kanchev, H.; Lu, D.; Colas, F.; Lazarov, V.; Francois, B. Energy Management and Operational Planning of a Microgrid with a PV-Based Active Generator for Smart Grid Applications. *IEEE Trans. Ind. Electron.* **2011**, *58*, 4583–4592. [[CrossRef](#)]
8. Miceli, R.; Viola, F. Designing a Sustainable University Recharge Area for Electric Vehicles: Technical and Economic Analysis. *Energies* **2017**, *10*, 1604. [[CrossRef](#)]
9. Clement-Nyns, K.; Haesen, E.; Driesen, J. The Impact of Charging Plug-In Hybrid Electric Vehicles on a Residential Distribution Grid. *IEEE Trans. Power Syst.* **2010**, *25*, 371–380. [[CrossRef](#)]
10. Kim, J.; Kim, S.W.; Jin, Y.G.; Park, J.-K.; Yoon, Y.T. Optimal Coordinated Management of a Plug-In Electric Vehicle Charging Station under a Flexible Penalty Contract for Voltage Security. *Energies* **2016**, *9*, 538. [[CrossRef](#)]
11. Shaaban, M.F.; Atwa, Y.M.; El-Saadany, E.F. PEVs modeling and impacts mitigation in distribution networks. *IEEE Trans. Power Syst.* **2013**, *28*, 1122–1131. [[CrossRef](#)]
12. Hung, D.Q.; Dong, Z.Y.; Trinh, H. Determining the size of PHEV charging stations powered by commercial grid-integrated PV systems considering reactive power support. *Appl. Energy* **2016**, *183*, 160–169. [[CrossRef](#)]
13. Kisacikoglu, M.C.; Erden, F.; Erdogan, N. Distributed Control of PEV Charging Based on Energy Demand Forecast. *IEEE Trans. Ind. Inform.* **2018**, *14*, 332–341. [[CrossRef](#)]
14. Carpinelli, G.; Mottola, F.; Proto, D.; Varilone, P. Minimizing unbalances in low-voltage microgrids: Optimal scheduling of distributed resources. *Appl. Energy* **2017**, *191*, 170–182. [[CrossRef](#)]
15. Li, Q.; Huang, M.; Zhang, W.; Bao, Y. Economic study on bus fast charging station with battery energy storage system. In Proceedings of the IEEE Transportation Electrification Conference and Expo, Asia-Pacific (ITEC Asia-Pacific), Harbin, China, 7–10 August 2017.
16. Di Giorgio, A.; Liberati, F.; Germana, R.; Presciuttini, M.; Celsi, L.R.; Delli Priscoli, F. On the control of energy storage systems for electric vehicles fast charging in service areas. In Proceedings of the Mediterranean Conference on Control and Automation (MED), Athens, Greece, 21–24 June 2016.
17. García-Triviño, P.; Fernández-Ramírez, L.M.; Torreglosa, J.P.; Jurado, F. Control of electric vehicles fast charging station supplied by PV/energy storage system/grid. In Proceedings of the IEEE International Energy Conference (ENERGYCON), Leuven, Belgium, 4–8 April 2016.
18. García-Triviño, P.; Torreglosa, J.P.; Fernández-Ramírez, L.M.; Jurado, F. Control and operation of power sources in a medium-voltage direct-current microgrid for an electric vehicle fast charging station with a photovoltaic and a battery energy storage system. *Energy* **2016**, *115*, 38–48. [[CrossRef](#)]
19. Thomas, D.; Deblecker, O.; Ioakimidis, C.S. Optimal operation of an energy management system for a grid-connected smart building considering photovoltaics' uncertainty and stochastic electric vehicles' driving schedule. *Appl. Energy* **2018**, *210*, 1188–1206. [[CrossRef](#)]
20. Mauri, G.; Valsecchi, A. Fast charging stations for electric vehicle: The impact on the MV distribution grids of the Milan metropolitan area. In Proceedings of the IEEE International Energy Conference and Exhibition (ENERGYCON), Florence, Italy, 9–12 September 2012.
21. Goli, P.; Shireen, W. PV powered smart charging station for PHEVs. *Renew. Energy* **2014**, *66*, 280–287. [[CrossRef](#)]
22. Sarker, M.R.; Pandžić, H.; Sun, K.; Ortega-Vazquez, M.A. Optimal operation of aggregated electric vehicle charging stations coupled with energy storage. *IET Gener. Trans. Distrib.* **2018**, *12*, 1127–1136. [[CrossRef](#)]

23. Ding, H.; Hu, Z.; Song, Y. Value of the energy storage system in an electric bus fast charging station. *Appl. Energy* **2015**, *157*, 630–639. [CrossRef]
24. Zhang, B.; Yan, Q.; Kezunovic, M. Placement of EV charging stations integrated with PV generation and battery storage. In Proceedings of the Twelfth International Conference on Ecological Vehicles and Renewable Energies (EVER), Monte Carlo, Monaco, 11–13 April 2017.
25. Negarestani, S.; Fotuhi-Firuzabad, M.; Rastegar, M.; Rajabi-Ghahnavieh, A. Optimal Sizing of Storage System in a Fast Charging Station for Plug-in Hybrid Electric Vehicles. *IEEE Trans. Transp. Electrification* **2016**, *2*, 443–453. [CrossRef]
26. Yuan, R.; Li, Q.; Zhong, K.; Jiang, Z.; Yin, Q.; Zhang, W. Research on the optimal capacity configuration of the energy storage system for an electric vehicle fast-charging station. In *Electromechanical Control Technology and Transportation, Proceedings of the 2nd International Conference on Electromechanical Control Technology and Transportation (ICECTT 2017), Zhuhai, China, 14–15 January 2017*; CRC Press: London, UK, 2017; p. 255.
27. Alharbi, W.; Bhattacharya, K. Electric Vehicle Charging Facility as a Smart Energy Microhub. *IEEE Trans. Sustain. Energy* **2017**, *8*, 616–628. [CrossRef]
28. Marra, F.; Yang, G.Y.; Træholt, C.; Larsen, E.; Østergaard, J.; Blažič, B.; Deprez, W. EV Charging Facilities and Their Application in LV Feeders With Photovoltaics. *IEEE Trans. Smart Grid* **2013**, *4*, 1533–1540. [CrossRef]
29. Islam, M.S.; Nadarajah, M.; Lee, K.Y. Suitability of PV and Battery Storage in EV Charging at Business Premises. *IEEE Trans. Power Syst.* **2017**, in press. [CrossRef]
30. Ugirumurera, J.; Haas, Z.J. Optimal Capacity Sizing for Completely Green Charging Systems for Electric Vehicles. *IEEE Trans. Transp. Electrification* **2017**, *3*, 565–577. [CrossRef]
31. Kandil, S.M.; Farag, H.E.Z.; Shaaban, M.F.; El-Sharafy, M.Z. A combined resource allocation framework for PEVs charging stations, renewable energy resources and distributed energy storage systems. *Energy* **2018**, *143*, 961–972. [CrossRef]
32. Shao, S.; Jahanbakhsh, F.; Agüero, J.R.; Xu, L. Integration of PEVs and PV-DG in power distribution systems using distributed energy storage—Dynamic analyses. In Proceedings of the IEEE PES Innovative Smart Grid Technologies Conference (ISGT), Washington, DC, USA, 24–27 February 2013.
33. Abronzini, U.; Attianese, C.; D’Arpino, M.; Di Monaco, M.; Genovese, A.; Pede, G.; Tomasso, G. Multi-source power converter system for EV charging station with integrated ESS. In Proceedings of the IEEE International Forum on Research and Technologies for Society and Industry Leveraging a Better Tomorrow (RTSI), Turin, Italy, 16–18 September 2015.
34. Silva, C.; Sousa, D.M.; Roque, A. Charging electric vehicles from photovoltaic generation with intermediate energy storage. In Proceedings of the International Conference on Clean Electrical Power (ICCEP), Santa Margherita Ligure, Italy, 27–29 June 2017.
35. Rubino, L.; Capasso, C.; Veneri, O. Review on plug-in electric vehicle charging architectures integrated with distributed energy sources for sustainable mobility. *Appl. Energy* **2017**, *207*, 438–464. [CrossRef]
36. Shivakumar, A.; Normark, B.; Welsch, M. Household DC Networks: State of the Art and Future Prospects. 2015. Available online: http://www.innoenergy.com/wp-content/uploads/2016/03/RREB7_DCnetworks_Final.pdf (accessed on 12 March 2018).
37. Elsayed, A.T.; Mohamed, A.A.; Mohammed, O.A. DC microgrids and distribution systems: An overview. *Electr. Power Syst. Res.* **2015**, *119*, 407–417. [CrossRef]
38. Yilmaz, M.; Krein, P.T. Review of Battery Charger Topologies, Charging Power Levels, and Infrastructure for Plug-In Electric and Hybrid Vehicles. *IEEE Trans. Power Electron.* **2013**, *28*, 2151–2169. [CrossRef]
39. Concept Study on Fast Charging Station Design. January 2016. Available online: http://www.edison-net.dk/Dissemination/Reports/Report_007.aspx (accessed on 12 March 2018).
40. Fantauzzi, M.; Lauria, D.; Mottola, F.; Scalfati, A. Sizing energy storage systems in DC networks: A general methodology based upon power losses minimization. *Appl. Energy* **2017**, *187*, 862–872. [CrossRef]
41. Ross, S. *Simulation*, 5th ed.; Academic Press: Cambridge, MA, USA, 2013.
42. Papoulis, A. *Probability, Random Variables and Stochastic Process*; McGraw-Hill: New York, NY, USA, 1991.
43. Chiodo, E.; Mazzanti, G. Mathematical and Physical Properties of Reliability Models in View of their Application to Modern Power System Components. In *Innovations in Power Systems Reliability*; Springer: London, UK, 2011.

44. Xiao, H.; Pei, W.; Dong, Z.; Kong, L.; Wang, D. Application and Comparison of Metaheuristic and New Metamodel Based Global Optimization Methods to the Optimal Operation of Active Distribution Networks. *Energies* **2018**, *11*, 85. [[CrossRef](#)]
45. Ul-Haq, A.; Cecati, C.; El-Saadany, E. Probabilistic modeling of electric vehicle charging pattern in a residential distribution network. *Electr. Power Syst. Res.* **2018**, *157*, 126–133. [[CrossRef](#)]
46. Ul-Haq, A.; Azhar, M.; Mahmoud, Y.; Perwaiz, A.; Al-Ammar, E.A. Probabilistic Modeling of Electric Vehicle Charging Pattern Associated with Residential Load for Voltage Unbalance Assessment. *Energies* **2017**, *10*, 1351. [[CrossRef](#)]
47. Bolognani, S.; Zampieri, S. On the Existence and Linear Approximation of the Power Flow Solution in Power Distribution Networks. *IEEE Trans. Power Syst.* **2016**, *31*, 163–172. [[CrossRef](#)]
48. Papathanassiou, S.; Hatziargyriou, N.; Strunz, K. A benchmark low voltage microgrid network. In Proceedings of the Cigre Symposium Power Systems with Dispersed Generation, Athens, Greece, 17–20 April 2005.



© 2018 by the authors. Licensee MDPI, Basel, Switzerland. This article is an open access article distributed under the terms and conditions of the Creative Commons Attribution (CC BY) license (<http://creativecommons.org/licenses/by/4.0/>).